Analytical and Bioanalytical Chemistry
https://doi.org/10.1007/s00216-019-02058-9

RESEARCH PAPER

A label-free photoelectrochemical DNA biosensor using a quantum dot–dendrimer nanocomposite

Faten Divsar[1]

Received: 3 June 2019 / Revised: 16 July 2019 / Accepted: 30 July 2019

Abstract

A novel label-free photoelectrochemical biosensing method for highly sensitive and specific detection of DNA hybridization using a CdS quantum dot (QD)–dendrimer nanocomposite is presented. A molecular beacon (MB) was assembled on a gold-nanoparticle-modified indium tin oxide electrode surface. Hybridization to a complementary target DNA disrupts the stem–loop structure of the MB, which was afterward labeled with the QD–dendrimer nanocomposite. The modified indium tin oxide electrode showed a stable anodic photocurrent response at 300 mV (vs Ag/AgCl) to light excitation at 410 nm in the presence of 0.1 M ascorbic acid as an electron donor. The protocol developed integrates the specificity of an MB for molecular recognition and the advantages of gold nanoparticles for increasing the loading capacity of the MB on the electrode surface and accelerating the electron transfer. Moreover, the photocurrent was greatly enhanced because of the high loading of QDs by the dendrimer, which eliminated the surface defects of CdS QDs and prevented recombination of their photogenerated electron–hole pairs. Under the optimal conditions, a linear relationship between the increase of photocurrent and target DNA concentration was obtained in the range from 1 fM to 0.1 nM, with a detection limit of 0.5 fM. The sequence-specificity experiment showed that one or three mismatches of DNA bases could be discriminated. This photoelectrochemical method is a prospective technique for DNA hybridization detection because of its great advantages: label-free, high sensitivity and specificity, low cost, and easy fabrication. This could create a new platform for the application of CdS QD–dendrimer nanocomposites in photoelectrochemical bioanalysis.

Keywords Poly(amidoamine) dendrimer · Quantum dots · Nanocomposites · Photoelectrochemical biosensor

Introduction

Sensitive real-time DNA assaying is critical to understand the genetic basis of disease and in cancer diagnostics and treatment [1, 2]. Methods that are quick and simple to detect and measure nucleic acids are preferable. Many analytical methods have been used for DNA detection, such as electrochemistry [3, 4], luminescence detection [5–8], colorimetry [9, 10], and surface plasmon resonance detection [11]. The large number of methods for the recognition of nucleic acid sequences is coupled with complicated fluorescence detection technology [12]. However, fluorescence-based assays have the disadvantage of high cost owing to the complex and expensive optical detection instrumentation.

The photoelectrochemical detection method is a newly developed method and is promising for a rapid and high-throughput biological assay [13] that is expected to have the advantages of both fluorescence and electrochemical sensors [14]. This method was used to detect and identify the sequence of the target DNA [15–18]. However, in the photoelectrochemical detection process, light is used to excite photoelectrochemically active species, and the photocurrent generated is used to detect the analyte. Because of the different forms of energy for excitation and detection, this process can reduce some background signals; therefore, its sensitivity is potentially high [19]. Additionally, it has some other notable advantages, such as electronic readout, easy fabrication, and potential applications in integrated microarray chips.

Electronic supplementary material The online version of this article (https://doi.org/10.1007/s00216-019-02058-9) contains supplementary material, which is available to authorized users.

✉ Faten Divsar
divsar@gmail.com

[1] Department of Chemistry, Payame Noor University, P.O. Box 19395-4697, Tehran, Iran

Published online: 10 August 2019

Semiconductor nanocrystals and quantum dots (QDs) such as TiO_2, SnO_2, Mn-doped CdS, CdTe, and CdS have been successfully used as photocurrent sensors because of their electronic structure and generation of electron–hole pairs during photoexcitation [20–25]. To enhance photocurrent generation, the retardation of the recombination of the photogenerated electron–hole pairs is essential. To maximize charge separation in semiconductor nanocrystals, different approaches have been suggested, including the use of hybrid composite semiconductor nanocrystals [26–28] or hybrid metal/semiconductor nanostructures [19, 29]. The assembly of CdS QD/carbon nanotube [30], CdSe QD/graphene [31], or TiO_2 semiconductor/carbon nanotube [32] hybrid systems was reported for the generation of high-quantum-yield photocurrents. When sufficiently long-lived electron–hole pairs are generated, this allows the ejection of conduction-band electrons to the electrode (anodic photocurrent) or the injection of electrons from the electrode into the valence band of the particle (cathodic photocurrent) [33]. However, the photocurrent can be greatly enhanced when electron donors or acceptors are present in solution.

TiO_2 nanoparticles possess a broad band gap and have photoelectrochemical activity under UV irradiation, which is damaging, whereas CdS QDs have a narrow band gap and are photoelectrochemically active in the visible range [34–37]. When CdS QDs absorb photons with energy greater than that of the band gap, electron–hole pairs are created. Once the process has occurred, the electron–hole pairs will recombine or the charges will be conveyed. Because of the lower energy level of the conduction band of indium tin oxide (ITO), the electrons are transferred to ITO, producing photocurrent [13]. However, it is imperative to find effective ways to enhance the photon-to-current conversion efficiency of semiconductor nanocrystals to develop improved photoelectrochemical biosensors.

Herein, a highly sensitive and label-free photoelectrochemical DNA biosensor based on a CdS QD–dendrimer nanocomposite is reported for the first time. Molecular beacons (MBs) were first assembled on a gold nanoparticle (AuNP)-modified ITO electrode. On hybridization to a complementary target, the MB stem–loop structure is disrupted and conjugates with the CdS QD–dendrimer nanocomposite. A photocurrent occurs because of the transfer of electrons from the CdS QDs into the conduction band of the ITO electrode. Ascorbic acid was used as an efficient and nontoxic donor of valence-band electrons of photoexcited CdS QDs in a mild solution medium. Poly(amidoamine) (PAMAM) dendrimers with amine surface groups, as hole acceptors, eliminate the surface-trapped electron–hole recombination, which enhances the photon-to-current conversion efficiency of CdS QDs [38]. Moreover, AuNPs are particularly advantageous for incrasing the loading capacity of the MB on the electrode surface and accelerating the electron transfer. In addition, the specificity of the MB for molecular recognition was used for the discrimination of complementary DNA from mismatched DNA. The method established could provide an approach for the assembly of CdS QD–dendrimer nanocomposites with other clinically important biomolecules to further the design of novel QD-based photoelectrochemical biosensors.

Methods

Materials

PAMAM (G4-NH_2, 4 wt% in methanol), cadmium nitrate, sodium sulfide, 3-mercaptopropionic acid (MPA; 99%), acetone, and methanol were purchased from Sigma-Aldrich and were used without further purification. Chloroauric acid ($HAuCl_4 \cdot 4H_2O$) and trisodium citrate were obtained from Shanghai Reagent Company (Shanghai, China). Glutaraldehyde (25% aqueous solution) and ascorbic acid were obtained from Sinopharm Chemical Reagent Co. (China). Labeled DNA oligonucleotides were synthesized by Shanghai Sangon Biotechnology Co. (Shanghai, China). Their sequences are given as follows:

- Hairpin DNA MB probe (17-base loop and 5-bp stem): 5′-SH-$(CH_2)_6$-TGGAGATCAGTCTGATAAGCTACTCCA-$(CH_2)_6$-NH_2-3′.
- Target: 5′-TAGCTTATCAGACTGAT-3′.
- One-base mismatch: 5′-TAGCTTAT**A**AGACTGAT-3′.
- Three-base mismatch: 5′-TAG**G**TTAT**A**AGAC**A**GAT-3′.

A 0.1 M phosphate buffer solution (PBS; pH 7.4) was prepared with NaH_2PO_4 and Na_2HPO_4 solution. PBS containing 0.1 M ascorbic acid was used as the electrolyte. All reagents were used as received. Double-distilled water was used throughout the experiments. ITO (N-STN-S1-10) with a coating thickness of 180 ± 20 nm and a sheet resistance of 8.1 ± 0.6 Ω/cm^{-2} was purchased from China Southern Glass Holding Co. (Shenzhen, China).

Apparatus

UV–visible absorption spectra were recorded with a Lambda 35 UV–visible spectrometer (PerkinElmer Instruments, Wellesley, MA, USA). Photoluminescence spectra were obtained with a JASCO FP 820 spectrofluorometer. Electrochemical impedance spectroscopy was performed with an Autolab potentiostat/galvanostat (PGSTAT30, Eco Chemie, Utrecht, Netherlands) in 0.1 M KCl containing a redox probe of 5.0 mM $K_3[Fe(CN)_6]/K_4[Fe(CN)_6]$ (1:1) at an open-circuit potential over a frequency range from

0.01 Hz to 10 kHz. Photoelectrochemical measurements were performed with a homemade photoelectrochemical system. A 500-W Xe lamp equipped with a monochromator was used as the irradiation source. Photocurrent was measured with a CHI 660D electrochemical workstation (CH Instruments, Austin, TX, USA). All experiments were performed at room temperature with a conventional three-electrode system with a modified ITO electrode as the working electrode, a platinum wire as the auxiliary electrode, and a saturated Ag/AgCl electrode as the reference electrode.

Synthesis of AuNPs

The AuNPs were prepared by citrate reduction of hydrogen tetrachloroaurate(III) in aqueous solution according to [39]. Briefly, an aqueous solution of $HAuCl_4$ (1%, 100 mL) was brought to reflux under stirring, and then 2 mL of a 1% trisodium citrate solution was added quickly, resulting in a change of solution color from pale yellow to deep red. After the color had changed, the solution was refluxed for an additional 10 min and was then allowed to cool to room temperature. The average size of the AuNPs was 13 nm (Fig. S1). The suspension obtained was kept in a refrigerator at 4 °C for future use.

Preparation of MPA-capped CdS QDs

Water-soluble CdS QDs were prepared according to a procedure described previously with some modifications [40]. Briefly, 2 mL of 5 mM $Cd(NO_3)_2$ solution and 5 mL of MPA were added to 25 mL of water and the pH was adjusted to 11 with 1 M NaOH before the addition of Na_2S under vigorous stirring. The final of Cd^{2+}/MPA/S^{2-} mole ratio was 1:2.5:0.5. During the aforementioned process, N_2 was bubbled through the solution for 30 min. The particle size was controlled by the quantity of Na_2S added as well as the temperature and duration of further heating. Thus, the sample was prepared by the addition of 1 mL of Na_2S and with stirring for 6 h at 100 °C under reflux. Low molecular weight contaminants were removed by dialysis against water. The final QD solution was stored in a refrigerator at 4 °C for future use.

Synthesis of the CdS QD–dendrimer nanocomposite

The nanocomposite was prepared by chemical reduction following a procedure reported previously with some modifications [41]. Firstly, a solution of cadmium ions was added to a solution of PAMAM dendrimers with a Cd^{2+}/dendrimer mole ratio of 10 and the mixture was vigorously stirred under nitrogen at 10 °C for about 30 min to make Cd^{2+} coordinate completely with PAMAM dendrimers. Then equimolar sodium sulfide was added to the aforementioned solution dropwise to obtain CdS QD nanocomposites. The low molecular weight contaminants were finally removed by dialysis against water. The suspension obtained was stored in a refrigerator at 4 °C for future use.

Fabrication of the photoelectrochemical DNA biosensor

The ITO slices as the working electrodes were cleaned by sonication in NaOH (1 M) and acetone, followed by washing with copious water and drying at 120 °C.

An even film of AuNPs was immobilized on the ITO electrode surface with use of 10 μL of 5 mM MPA followed by 20 μL AuNPs after 1 h incubation, resulting in the formation of a classic alkanethiol–gold linkage. Then 10 μL of the thiolated MB probe was spread on the AuNP film for 1 h incubation. Subsequently, a solution of target DNA oligonucleotides was incubated on the electrode for 70 min to form double-stranded DNA. Conjugation of CdS QD–dendrimer nanocomposites to the MB-modified electrode was achieved with use of glutaraldehyde for the classic coupling reaction between surface amine groups of the dendrimer and amine groups of the MB. For this, 20 μL of CdS QD–dendrimer nanocomposite solution was dropped on the electrode surface. All these incubation steps were performed at room temperature. The whole preparation process is outlined in Fig. 1. Before measurement, the biosensor was washed with PBS to remove physically absorbed nanocomposites. The corresponding electrode was in contact with 0.1 M PBS (pH 7.4) containing 0.1 M ascorbic acid and was scanned with potential of 300 mV at 410 nm.

Results and discussion

Characterization of the CdS QD–dendrimer nanocomposite

Photoluminescence and UV–visible absorption spectra were used to characterize the synthesized CdS QD–dendrimer nanocomposite (Fig. S2). The CdS QD–dendrimer nanocomposite and MPA-capped CdS QDs showed photoluminescence peaks at 538 and 550 nm, respectively, and absorption peaks at 354 and 370 nm, respectively, indicating the consequence of quantum confinement [42]. The morphology of the CdS QD–dendrimer nanocomposite and that of the MPA-capped CdS QDs were obtained by transmission electron microscopy. The images show spherical and monodisperse particles for both the CdS QD–dendrimer nanocomposite and MPA-capped CdS QDs. The size of the CdS QDs was about 2 nm for the CdS QD–dendrimer nanocomposite and about 3 nm for the MPA-capped CdS QDs

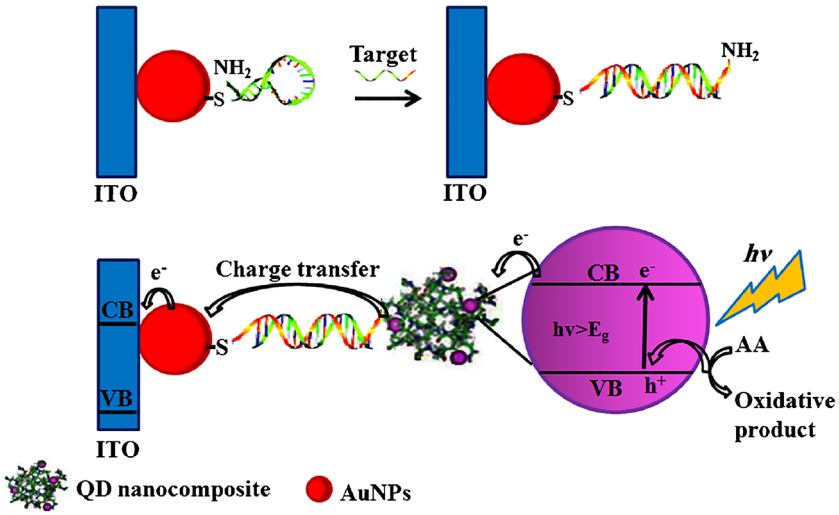

Fig. 1 The biosensor fabrication process and its anodic photocurrent generation mechanism. AA ascorbic acid, AuNP gold nanoparticle, CB conduction band, ITO indium tin oxide, QD quantum dot, VB valence band

(Fig. 2). The sizes of the resulting QDs and the concentration of QD suspensions were also estimated from the absorption maximum in the UV–visible spectra and the empirical equation reported previously [43].

$$D = \left(-6.6521 \times 10^{-8}\right)\lambda^3 + \left(1.9557 \times 10^{-4}\right)\lambda^2 - \left(9.2352 \times 10^{-2}\right)\lambda + (13.29), \quad (1)$$

$$\varepsilon = 21536D^{2.3}, \quad (2)$$

where D (nm) is the size of nanocrystals, λ (nm) is the wavelength of their first excitonic absorption peak, and ε is the extinction coefficient per mole of nanocrystals (L/mol cm). The concentration of nanocrystals in solution was calculated with the Lambert-Beer law. The sizes of the CdS QDs in the CdS QD–dendrimer nanocomposite and the MPA-capped CdS QDs were calculated to be 2.15 and 2.52 nm, respectively, with concentrations of 5.99 and 1.88 μM, respectively.

Electrochemical impedance spectroscopy and photoelectrochemical characterization of the biosensor

Electrochemical impedance spectroscopy is an effective method to monitor the features of modified electrode surfaces. Figure 3 shows the electrochemical impedance Nyquist plot of different modified electrodes with $K_3[Fe(CN)_6]$/$K_4[Fe(CN)_6]$ as the redox probe in 0.1 M potassium chloride solution (pH 7.4) with an alternating voltage of 5 mV and a frequency range of 0.01 Hz to 10 kHz. Compared with the bare ITO electrode (curve a), the MPA-modified electrode showed a larger diameter of the frequency semicircle (curve b), which was due to the insulating effect of MPA. When the ITO/MPA electrode was modified with AuNPs, the diameter of the Nyquist circle decreased (curve c), which is attributed to the increase of electron transfer. This indicates that an AuNP layer was successfully formed on the electrode surface. Subsequently, immobilization of the MB on the AuNP-modified electrode increased the resistance (curve d), which

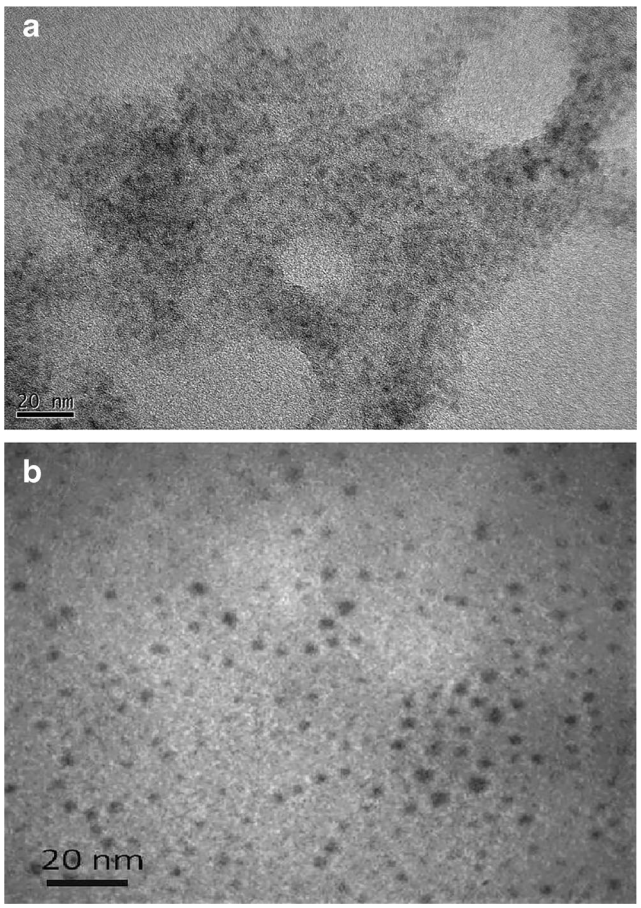

Fig. 2 Transmission electron microscopy images of **a** CdS quantum dot (QDs)–dendrimer nanocomposite and **b** 3-mercaptopropionic acid-capped CdS QDs

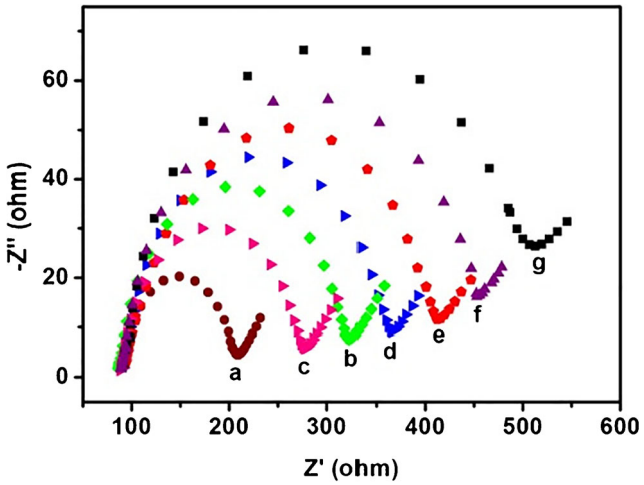

Fig. 3 Electrochemical impedance Nyquist plots of (a) bare indium tin oxide (ITO), (b) ITO/3-mercaptopropionic acid (MPA), (c) ITO/MPA/gold nanoparticles (AuNPs), (d) ITO/MPA/AuNPs/molecular beacon (MB), (e) ITO/MPA/AuNPs/MB/10 pM target DNA, (f) ITO/MPA/AuNPs/MB/10 pM target DNA/glutaraldehyde, and (g) ITO/MPA/AuNPs/MB/10 fM target DNA/glutaraldehyde/quantum dot nanocomposite in 0.1 M phosphate buffer solution (pH 7.4) containing 0.1 M ascorbic acid. The excitation wavelength was 410 nm and the applied potential was 300 mV

means that the MB formed an additional barrier and further prevented the redox probe from approaching the electrode surface. The resistance increased again after 10 pM target DNA had conjugated to the MB (curve e). However, the diffusion resistance for electron motion increased in the thicker modified layer on the electrode surface. The electron transfer resistance was enhanced by means of glutaraldehyde and then CdS QD–dendrimer nanocomposite on the modified electrode (curves f and g). These results clearly confirm the successful modification of the electrode.

The fabrication of the biosensor was also monitored by photoelectrochemical experiments (Fig. 4). The sharp anodic photocurrent appeared at negative potential just after the final modification of the ITO electrode with the CdS QD–dendrimer nanocomposite. This indicates that the different multilayers on the electrode surface were not photoactive (curves a–d) and the electron transfer was caused only by the electron–hole pairs of CdS QDs (curve e). The current was relatively stable over time and could be turned on and off by our controlling the light. A control experiment was performed without target DNA, resulting in the MB stem–loop structure remaining closed and showing no photocurrent signal. This further proves that the photocurrent was due to the CdS QD–dendrimer nanocomposite.

Photoelectrochemical response of the biosensor

As shown in Fig. 5, the photocurrent intensity of the electrode modified with the CdS QDs–dendrimer nanocomposite (curve c) is much greater than that of the electrode modified with CdS QDs (curve a) in PBS (pH 7.4). This was attributed to the loading of numerous QDs by the PAMAM dendrimers and also the amine groups of PAMAM dendrimers reducing the surface defects of CdS QDs, which acted as the surface trapped electron–hole recombination [44]. The photoresponse of the modified electrodes increased when the ascorbic acid redox couple was present in solution (curves b and d). After the separation of electron–hole pairs, the holes migrate into solution, in which they oxidize the electron donor (ascorbic

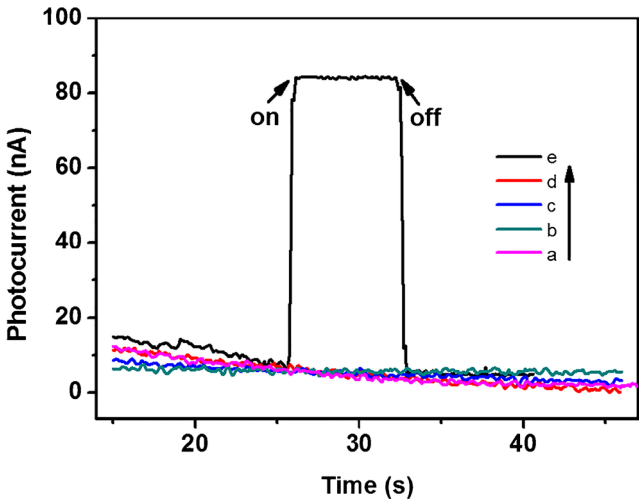

Fig. 4 Photocurrent response of (a) bare indium tin oxide (ITO), (b) ITO/3-mercaptopropionic acid (MPA)/gold nanoparticles (AuNPs), (c) ITO/MPA/AuNPs/molecular beacon (MB), (d) ITO/MPA/AuNPs/MB/10 fM target DNA, and (e) ITO/MPA/AuNPs/MB/10 fM target DNA/glutaraldehyde/quantum dot nanocomposite in 0.1 M phosphate buffer solution (pH 7.4) containing 0.1 M ascorbic acid. The excitation wavelength was 410 nm and the light was turned on and off as indicated. The applied potential was 300 mV

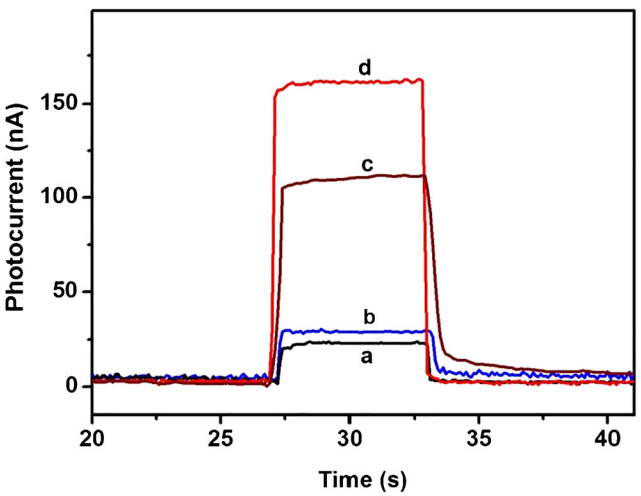

Fig. 5 Photocurrent responses to light excitation at 410 nm of modified indium tin oxide electrodes for 10 pM target DNA labeled with (a, b) CdS quantum dots (QDs) and (c, d) CdS QD–dendrimer nanocomposite in 0.1 M phosphate buffer solution (pH 7.4) in (a, c) the absence and (b, d) the presence of 0.1 M ascorbic acid at 300 mV

acid). If there are no ascorbic acid molecules in the detection solution, photogenerated electrons can recombine with holes and only a low photocurrent is generated.

The proposed mechanism for the electron transfer system is shown in Fig. 1. The photoexcitation of the CdS QDs causes the transfer of an electron from the occupied valence band to the empty conduction band, and hence produces an electron–hole pair. Whereas the luminescence features of the CdS QDs arise from electron–hole recombination, the trapping of conduction-band electrons in surface traps provides sufficiently long-lived electron–hole pairs that allow the ejection of the conduction-band electrons to electrodes, giving rise to photoelectrochemical current production. The ejection of the conduction-band electrons to the electrode, accompanying electron transfer from a water-soluble electron donor, generates an anodic photocurrent. The photocurrent can be switched on and off by pulsed irradiation of the QDs. The mechanism of photocurrent production possibly includes the photoejection of conduction-band electrons of CdS QDs in contact with or at tunneling distances from the electrode. AuNPs act as the charge source for helping the interfacial charge-transfer processes that increase the photocurrent intensity.

Effect of ascorbic acid concentration

As shown in Fig. S3, the photocurrent intensity of 1 pM target at an applied potential of 300 mV increased with the increase of the electron donor concentration and reached a maximum for 0.1 M ascorbic acid; a weak decline was detected for much higher concentrations of ascorbic acid. As a hole collector, ascorbic acid in lower concentrations resulted in a decrease in electrical productivity because there were fewer reducing agent molecules for electron donation to photogenerated holes, whereas much higher concentration of ascorbic acid would lead to enhancement of the absorbance of ascorbic acid in the solution, and consequently the amount of irradiation reaching the electrode surface decreased and the capability of excited QDs would be reduced [13].

Effect of QD nanocomposite amount

CdS QD–dendrimer nanocomposites as photoactive materials showed a quick photocurrent response to 410-nm photoexcitation. However, a large amount of QD nanocomposite can be loaded on the electrode surface, and therefore a larger photocurrent intensity can be obtained. To investigate the proper amount of QD nanocomposite as a label, the electrodes modified with 10 pM target DNA were labeled with different amounts of QD nanocomposite. From the resulting calibration curve (Fig. S4), the photocurrents increased with the amount of QD nanocomposite. This indicated that the QD nanocomposites were adsorbed increasingly during the assembly. However, a decreasing tendency in the photocurrents appeared with increasing amount of nanocomposite label exceeding 20 μL of nanocomposite suspension (0.12 nmol of QDs). The explanation might be that the thick film was subject to diffusion limitation between the inner portion of CdS QDs and the electron donor ascorbic acid when more QD nanocomposite was added on the electrode surface [13]. Thus, 20 μL of nanocomposite suspension was used for further experiments.

Effects of pH and incubation time on the electrode response

The pH effect of PBS on the biosensor response was studied in the range from 5.2 to 10.0 in the presence of 0.1 M ascorbic acid. The current response of 10 pM target DNA increased from pH 5.2 to pH 7.0 and was maximum at pH 7.4, and then decreased from pH 7.4 to pH 10.0 (Fig. S5). In the process, OH^- served as a hole scavenger [15], resulting in enhancement of charge separation and decrease of electron–hole pair recombination, thus resulting in an increase of photocurrent with pH increase. At pH higher than 7.4, the decrease was attributed to decrease of the concentration of H^+, which consumed the conduction-band electrons of QDs, resulting in the decrease of photocurrent. To obtain maximum sensitivity and bioactivity, pH 7.4 was chosen.

The influence of the incubation time on the photocurrent response was also studied. For this, hybridization was performed at 37 °C for various times and then the hybridized electrodes were rinsed with PBS (pH 7.4) to remove unbound DNA molecules. As shown in Fig. S6, the maximal photocurrent of 10 pM target DNA was obtained after incubation at 37 °C for 1 h, which was chosen as the optimal incubation time.

Effect of applied potential and wavelength on photocurrent

It is important to evaluate the dependence of photocurrent on the applied potential to understand the detailed photocurrent generation mechanism. The photocurrent of 10 pM target DNA increased gradually when the applied potential shifted from 0 to 400 mV and reached a maximum value at 300 mV (Fig. 6a). The increasing cathodic photocurrent with increasing negative potential indicates n-type behavior of the CdS QD–dendrimer nanocomposite where electrons migrate from the QDs to the ITO electrode. Afterward, the rate of increase decreased with unstable photocurrent and the electrode decomposed at 500 mV. As higher voltage would damage the DNA probe by oxidation of the Au–S bond [45], all the photoelectric experiments were consequently performed with an applied voltage less than this critical value. Therefore, for higher sensitivity, 300 mV was selected in this work.

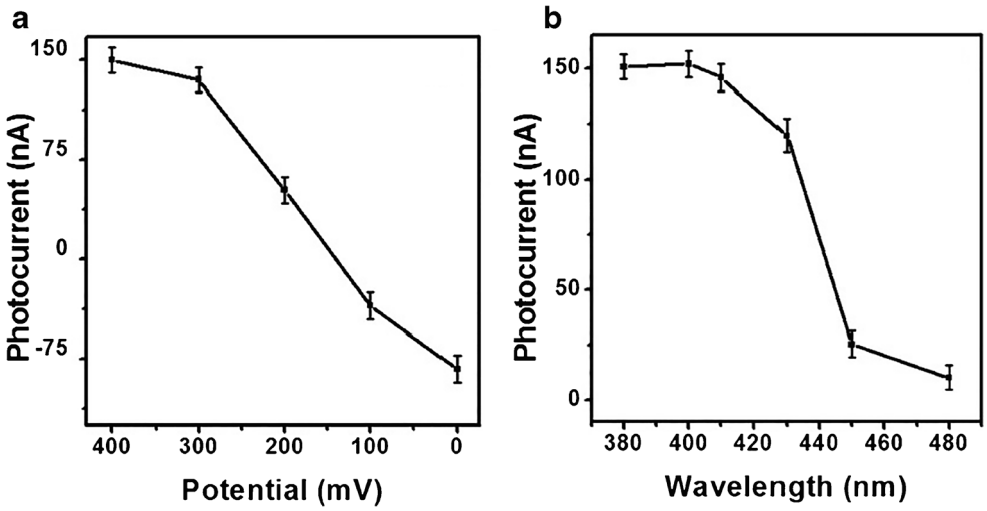

Fig. 6 Effects of **a** applied potential and **b** excitation wavelength on photocurrent response of the electrode modified with 10 pM target DNA in 0.1 M phosphate buffer solution (pH 7.4) containing 0.1 M ascorbic acid

Efficient photocurrent generation needs absorbed photons with energy greater than the band gap. The band gap energy of the CdS QDs is 2.6 eV, and the maximum wavelength to produce photocurrent was calculated to be about 477 nm. The photocurrent response of the modified ITO electrode with 10 pM target DNA was investigated from 380 to 480 nm (Fig. 6b). The modified electrode showed the strongest photocurrent intensity at around 390–410 nm. The increase was attributed to the absorption coefficient of the QDs, which increases with photon energy greater than the QD band gap energy [46]. More energetic photons can excite electrons from populated regions of the valence band to available states deep in the conduction band. However, 410 nm as a longer wavelength, which is favorable for monitoring of biological systems, was chosen for the following experiments.

Sensitivity and selectivity

Under the optimal conditions, the calibration graph obtained for the determination of different concentrations of target DNA without any amplification of its amount is shown in Fig. 7. The photocurrent increased in proportion to the logarithm of DNA target concentration in the range from 1 fM to 0.1 nM, with a detection limit of 0.5 fM and a correlation coefficient of 0.9916. The good linearity over a wide dynamic range suggested that the DNA target could be determined quantitatively with the proposed photoelectrochemical biosensor. The present work has demonstrated significantly increased sensitivity over previous methods for the detection of DNA in solution. The sensitivity of this biosensor is among the highest reported so far. The lowest detection limit of a photoelectrochemical DNA biosensor was reported to be 20 fM with a dynamic range from 50 fM to 1.0 nM [47], whereas a photocurrent system using a DNA intercalator on porous SnO_2 film showed a limit of detection 0.18 nM and a linear range from 0.5 to 7 nM [12]. A detection limit of 1 nM with a dynamic range from 1 to 500 nM was obtained with an AuNP-labeled DNA probe on a TiO_2 substrate [19] compared with a detection limit of 2.5 nM for an unlabeled one [15]. A photocurrent DNA biosensor with a chemiluminescence reaction as the light source showed a detection limit of 4.5 nM and a linear range from 20 to 400 nM [48]. It is noteworthy that the present work showed a detection limit about 40 times lower than the previous lowest one with about the same wide dynamic range. The relative standard deviations of five replicates of 1 and 100 pM were 8.2% and 4.9% respectively, indicating good reproducibility of the biosensor.

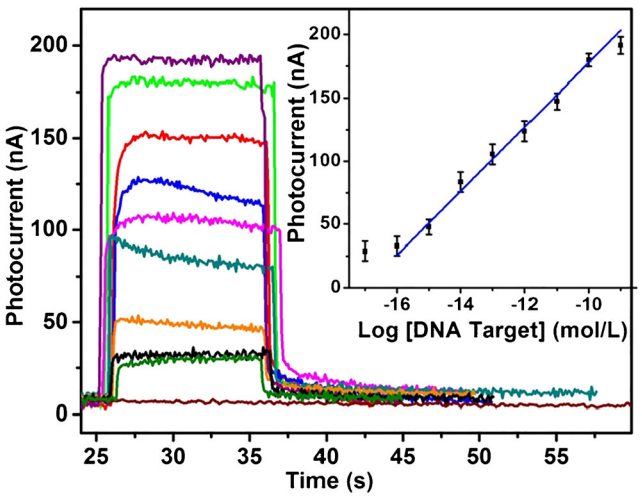

Fig. 7 Photocurrent responses to light excitation at 410 nm of the modified indium tin oxide electrode in 0.1 M phosphate buffer solution (pH 7.4) containing 0.1 M ascorbic acid for 0 fM, 0.01 fM, 0.1 fM, 1 fM 0.01 pM, 0.1 pM, 1 pM, 10 pM, 100 pM, and 1000 pM target DNA (from bottom to top) at 300 mV. The inset shows the linear calibration curve

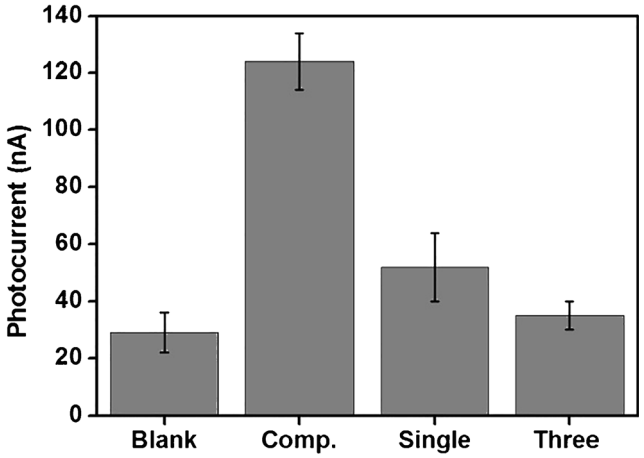

Fig. 8 Photocurrent responses obtained with the CdS quantum dot–G4 dendrimer nanocomposite for detection of 10 pM target DNA, single-base-mismatched sequence, and three-base-mismatched sequence. Comp. complementary

At the same concentration of 1 pM, single-base-mismatched, three-base-mismatched, and complementary DNA oligonucleotide solutions were used for hybridization and then the photocurrent of the modified electrodes was measured. Figure 8 shows that the signals from the single-base-mismatched and three-base-mismatched DNA were 41.9% and 28.2%, respectively, of the signal from the complementary DNA. This comparison demonstrates that this biosensor has high selectivity for the sequence-specific detection of the target DNA.

Conclusions

A unique label-free photoelectrochemical biosensor was developed for the quantification of DNA in solution. A CdS QD–dendrimer nanocomposite was used for the first time as a highly sensitive photoelectrochemical label, where PAMAM dendrimer eliminated the surface defects of CdS QDs and prevented recombination of their photogenerated electron–hole pairs. Moreover, it took advantage of AuNPs as electron transfer facilitators and also as MB anchors. Ascorbic acid as an electron donor in solution enhanced the photocurrent response of the modified electrode. The ultrahigh sensitivity of the biosensor described here allows the quantification of DNA without a preamplification step over a wide dynamic range. This strategy manifests its excellence by being simple, cost-effective, and specific, which allow it to be used as a high-throughput screening technique. It has a bright future for photoelectrochemical biosensors to study a wide variety of biological processes.

Compliance with ethical standards

Conflict of interest The author declare that she has no competing interests.

References

1. Lazcka O, Del Campo FJ, Munoz FX. Pathogen detection: a perspective of traditional methods and biosensors. Biosens Bioelectron. 2007;22:1205–17.
2. Palchetti I, Mascini M. Nucleic acid biosensors for environmental pollution monitoring. Analyst. 2008;133:846–54.
3. Chang HX, Yuan Y, Shi NL, Guan YF. Electrochemical DNA biosensor based on conducting polyaniline nanotube array. Anal Chem. 2007;79:5111–5.
4. Gore MR, Szalai VA, Ropp PA, Yang IV, Silverman JS, Thorp HH. Detection of attomole quantities [correction of quantitites] of DNA targets on gold microelectrodes by electrocatalytic nucleobase oxidation. Anal Chem. 2003;75:6586–92.
5. Divsar F, Ju HX. Electrochemiluminescence detection of near single DNA molecules by using quantum dots–dendrimer nanocomposites for signal amplification. Chem Commun. 2011;47:9879–81.
6. Kim HY, Kane MD, Kim S, Dominguez W, Applegate BM, Savikhin S. A molecular beacon DNA microarray system for rapid detection of E. coli O157:H7 that eliminates the risk of a false negative signal. Biosens Bioelectron. 2007;22:1041–7.
7. Wu ZS, Jiang JH, Fu L, Shen GL, Yu RQ. Optical detection of DNA hybridization based on fluorescence quenching of tagged oligonucleotide probes by gold nanoparticles. Anal Biochem. 2006;353:22–9.
8. Wang HB, Ou LJ, Huang KJ, Wen XG, Wang LL, Liu YM. A sensitive biosensing strategy for DNA detection based on graphene oxide and T7 exonuclease assisted target recycling amplification. Can J Chem. 2013;91:1266–71.
9. Elghanian R, Storhoff JJ, Mucic RC, Letsinger RL, Mirkin CA. Selective colorimetric detection of polynucleotides based on the distance-dependent optical properties of gold nanoparticles. Science. 1997;277:1078–81.
10. Storhoff JJ, Elghanian R, Mucic RC, Mirkin CA, Letsinger RL. One-pot colorimetric differentiation of polynucleotides with single base imperfections using gold nanoparticle probes. J Am Chem Soc. 1998;120:1959–64.
11. Ananthanawat C, Vilaivan T, Mekboonsonglarp W, Hoven VP. Thiolated pyrrolidinyl peptide nucleic acids for the detection of DNA hybridization using surface plasmon resonance. Biosens Bioelectron. 2009;24:3544–9.
12. Liu S, Li C, Cheng J, Zhou Y. Selective photoelectrochemical detection of DNA with high-affinity metallointercalator and tin oxide nanoparticle electrode. Anal Chem. 2006;78:4722–6.
13. Wang GL, Yu PP, Xu JJ, Chen HY. A label-free photoelectrochemical immunosensor based on water-soluble Cds quantum dots. J Phys Chem C. 2009;113:11142–8.
14. Ikeda A, Nakasu M, Ogasawara S, Nakanishi H, Nakamura M, Kikuchi JI. Photoelectrochemical sensor with porphyrin-deposited electrodes for determination of nucleotides in water. Org Lett. 2009;11:1163–6.
15. Lu W, Wang G, Jin Y, Yao X, Hu JQ, Li JH. Label-free photoelectrochemical strategy for hairpin DNA hybridization detection on titanium dioxide electrode. Appl Phys Lett. 2006;89:263902.
16. Lu W, Jin Y, Wang G, Chen D, Li JH. Enhanced photoelectrochemical method for linear DNA hybridization detection using Au-nanopaticle labeled DNA as probe onto titanium dioxide electrode. Biosens Bioelectron. 2008;23:1534–9.
17. Tokudome H, Yamada Y, Sonezaki S, Ishikawa H, Bekki M, Kanehira K, et al. Photoelectrochemical deoxyribonucleic acid sensing on a nanostructured TiO_2 electrode. Appl Phys Lett. 2005;87:213901.

18. Willner I, Patolsky F, Wasserman J. Photoelectrochemistry with controlled DNA-cross-linked CdS nanoparticle arrays. Angew Chem. 2001;113:1913–6.
19. Wang GL, Xu JJ, Chen HY. Progress in the studies of photoelectrochemical sensors. Sci China Ser B. 2009;52:1789–800.
20. Wang B, Dong YX, Wang YL, Cao JT, Ma SH, Liu YM. Quenching effect of exciton energy transfer from CdS:Mn to Au nanoparticles: a highly efficient photoelectrochemical strategy for microRNA-21 detection. Sensors Actuators B Chem. 2018;254:159–65.
21. Fan GC, Zhu H, Du D, Zhang J, Zhu JJ, Lin Y. Enhanced photoelectrochemical immunosensing platform based on CdSeTe@CdS:Mn core-shell quantum dots sensitized TiO_2 amplified by CuS nanocrystals conjugated signal antibodies. Anal Chem. 2016;88:3392–9.
22. Dong YX, Cao JT, Wang B, Ma SH, Liu YM. Exciton−plasmon interactions between CdS@g-C_3N_4 heterojunction and Au@Ag nanoparticles coupled with DNAase-triggered signal amplification: Toward highly sensitive photoelectrochemical bioanalysis of microRNA. ACS Sustain Chem Eng. 2017;5:10840–8.
23. Dastan D, Panahi SL, Chaure NB. Characterization of titania thin films grown by dip-coating technique. J Mater Sci Mater Electron. 2016;27:12291–6.
24. Dastan D, Panahi SL, Yengntiwar AP, Banpurkar AG. Morphological and electrical studies of titania powder and films grown by aqueous solution method. Adv Sci Lett. 2016;22:950–3.
25. Panahi SL, Dastan D, Chaure NB. Characterization of zirconia nanoparticles grown by sol-gel method. Adv Sci Lett. 2016;22:941–4.
26. Nasr C, Hotchandani S, Kim WY, Schmehl RH, Kamat PV. Photoelectrochemistry of composite semiconductor thin films. Photosensitization of SnO_2/CdS coupled nanocrystallites with a ruthenium polypyridyl complex. J Phys Chem B. 1997;101:7480–7.
27. Shen Q, Ayuzawa Y, Katayama K, Sawada T, Toyoda T. Separation of ultrafast photoexcited electron and hole dynamics in CdSe quantum dots adsorbed onto nanostructured TiO_2 films. Appl Phys Lett. 2010;97:263113.
28. Zhao WW, Yu PP, Xu JJ, Chen HY. Ultrasensitive photoelectrochemical biosensing based on biocatalytic deposition. Electrochem Commun. 2011;13:495–7.
29. Sheeney-Haj-Ichia L, Pogorelova S, Gofer Y, Willner I. Enhanced photoelectrochemistry in CdS/Au nanoparticle bilayers. Adv Funct Mater. 2004;14:416–24.
30. Sheeney-Haj-Ichia L, Basnar B, Willner I. Efficient generation of photocurrents by using CdS/carbon nanotube assemblies on electrodes. Angew Chem Int Ed. 2005;44:78–83.
31. Zhang X, Li S, Jin X, Zhang S. A new photoelectrochemical aptasensor for the detection of thrombin based on functionalized graphene and CdSe nanoparticles multilayers. Chem Commun. 2011;47:4929–31.
32. Kongkanand A, Domínguez RM, Kamat PV. Single wall carbon nanotube scaffolds for photoelectrochemical solar cells. Capture and transport of photogenerated electrons. Nano Lett. 2007;7:676–80.
33. Gill R, Zayats M, Willner I. Semiconductor quantum dots for bioanalysis. Angew Chem Int Ed. 2008;47:7602–25.
34. Tu WW, Dong Y, Lei JP, Ju HX. Low-potential photoelectrochemical biosensing using porphyrin-functionalized TiO_2 nanoparticles. Anal Chem. 2010;82:8711–6.
35. Dastan D, Chaure N, Kartha M. Surfactants assisted solvothermal derived titania nanoparticles: synthesis and simulation. J Mater Sci Mater Electron. 2017;28:7784–96.
36. Dastan D. Effect of preparation methods on the properties of titania nanoparticles: solvothermal versus sol-gel. Appl Phys A Mater Sci Process. 2017;123:1–13.
37. Dastan D, Banpurkar A. Solution processable sol-gel derived titania gate dielectric for organic field effect transistors. J Mater Sci Mater Electron. 2016;28:3851–9.
38. Qian Z, Bai HJ, Wang GL, Xu JJ, Chen HY. A photoelectrochemical sensor based on CdS-polyamidoamine nanocomposite film for cell capture and detection. Biosens Bioelectron. 2010;25:2045–50.
39. Grabar KC, Freeman RG, Hommer MB, Natan MJ. Preparation and characterization of Au colloid monolayers. Anal Chem. 1995;67:735–43.
40. Priyam A, Chatterjee A, Das SK, Saha A. Synthesis and spectral studies of cysteine-capped CdS nanoparticles. Res Chem Intermed. 2005;31:691–702.
41. Jin YJ, Luo YJ, Li GP, Li J, Wang YF, Yang RQ, et al. Application of photoluminescent CdS/PAMAM nanocomposites in fingerprint detection. Forensic Sci Int. 2008;179:34–8.
42. Murray CB, Norris DJ, Bawendi MG. Synthesis and characterization of nearly monodisperse CdE (E = sulfur, selenium, tellurium) semiconductor nanocrystallites. J Am Chem Soc. 1993;115:8706–15.
43. Yu WW, Qu LH, Guo WZ, Peng XG. Experimental determination of the extinction coefficient of CdTe, CdSe, and CdS nanocrystals. Chem Mater. 2003;15:2854–60.
44. Zhang CX, O'Brien S, Balogh L. Comparison and stability of CdSe nanocrystals covered with amphiphilic poly(amidoamine) dendrimers. J Phys Chem B. 2002;106:10316–21.
45. Qingwen L, Guoan L, Jun F, Dawen C, Qi O. Photoelectrochemistry as a novel strategy for DNA hybridization detection. Analyst. 2000;125:1908–10.
46. Street RA, Qi P, Lujan R, Wong WS. Reflectivity of disordered silicon nanowires. Appl Phys Lett. 2008;93:163109.
47. Gao Z, Tansil NC. An ultrasensitive photoelectrochemical nucleic acid biosensor. Nucleic Acids Res. 2005;33:e123.
48. Zhang X, Zhao Y, Zhou H, Qu B. A new strategy for photoelectrochemical DNA biosensor using chemiluminescence reaction as light source. Biosens Bioelectron. 2011;26:2737–41.